

# Estimating Shapley effects for moderate-to-large input dimensions <sup>\*</sup>

Akira Horiguchi<sup>†</sup> and Matthew T. Pratola<sup>‡</sup>

**Abstract.** Sobol’ indices and Shapley effects are attractive methods of assessing how a function depends on its various inputs. The existing literature contains various estimators for these two classes of sensitivity indices, but few estimators of Sobol’ indices and no estimators of Shapley effects are computationally tractable for moderate-to-large input dimensions. This article provides a Shapley-effect estimator that is computationally tractable for a moderate-to-large input dimension. The estimator uses a metamodel-based approach by first fitting a Bayesian Additive Regression Trees model which is then used to compute Shapley-effect estimates. This article also establishes posterior contraction rates on a large function class for this Shapley-effect estimator and for the analogous existing Sobol’-index estimator. Finally, this paper explores the performance of these Shapley-effect estimators on four different test functions for moderate-to-large input dimensions and number of observations.

**Key words.** Nonparametric, functional ANOVA, global sensitivity analysis, variable importance, surrogate model

**MSC codes.** 62G20, 62G08

**1. Introduction.** An important task in global sensitivity analysis is to measure how a function depends on its various inputs. A popular measure of variable importance is the class of Sobol’ indices [1], which decomposes the variance of outputs from a function into terms due to main effects for each input and interaction effects between the various inputs. To quantify the impact of any particular input dimension, either the *main-effect Sobol’ index* or the *total-effect Sobol’ index* can be used; the latter includes all interactions between the given input and any other input whereas the former excludes any such interaction. Intuitive interpretation of Sobol’ indices requires an orthogonal distribution on the inputs [2]. *Shapley effects* [2, 3] form another class of variance-based global sensitivity indices that was first introduced in the context of game theory but has only recently been gaining traction in the statistics literature [4]. Although the additional computation required to compute Shapley effects might render them unnecessary if the inputs are known to be independent, Shapley effects remain interpretable even if the inputs are correlated [2] and hence are the more reasonable option in such a case.

A function’s Sobol’ indices and Shapley values can, on occasion, be computed exactly, particularly when a closed-form expression of the function is known and the required expectations can be computed easily. But more often than not, computing these expectations requires some sort of integral approximation. Monte Carlo integration is a simple option and is used to estimate Shapley effects by e.g. [2, 5, 6, 7], but computation becomes intractable as the

\*

**Funding:** The work of MTP was supported in part by the National Science Foundation under Agreements DMS-1916231, OAC-2004601, and in part by the King Abdullah University of Science and Technology (KAUST) Office of Sponsored Research (OSR) under Award No. OSR-2018-CRG7-3800.3.

<sup>†</sup>Department of Statistical Science, Duke University, Durham, NC ([akira.horiguchi@duke.edu](mailto:akira.horiguchi@duke.edu)).

<sup>‡</sup>Department of Statistics, The Ohio State University, Columbus, OH ([mpratola@stat.osu.edu](mailto:mpratola@stat.osu.edu)).

number of inputs increases. Another option is to first fit a metamodel which can then be used to compute estimates of Sobol' indices and Shapley effects as a post-processing step. This approach is also useful when a function can only be sparsely evaluated, necessitating the use of a metamodel. A popular metamodel fit for this purpose is the Gaussian Process (GP) model. Chapter 7 of [8] notes that the required expectations are known for GPs with polynomial mean and either a separable Gaussian, Bohman, or cubic correlation function [9, 10, 11, 12, 13, 14]. [15] use GPs to compute Shapley effects in a simulation study with a three-dimensional input space. Other metamodels used to compute Sobol' indices include generalized polynomial chaos expansions [16], treed GPs [17], dynamic trees [18], Gaussian radial basis function [19], artificial neural networks [20], Bayesian multivariate adaptive regression splines [21], and deep GPs [22]. However, many of these metamodel-based approaches struggle to either fit the metamodel or compute the Sobol'-index estimates if the number of inputs and function evaluations is moderate-to-large.

In addition to these computational challenges, the existing literature contains few theoretical guarantees of contraction rates for estimators of Sobol' indices. [23] propose an asymptotically efficient estimator for sensitivity indices that include Sobol' indices as a special case, but this efficiency result assumes a one-dimensional input space and the existence of an estimator of the joint density of the input-output pair that converges quickly enough to the true joint density. [24] establish central limit theorems (CLTs) for two Sobol' index estimators. [25] establish a CLT for a rank-based estimator of first-order Sobol' indices, where the CLT result requires the boundedness of either the function  $f_0$  and its two first derivatives with respect to each of its coordinates, or that  $f_0 \circ F_j^{-1}$  and its two first derivatives are bounded, where  $F_j$  is the cumulative distribution function of the  $j$ th input dimension. Finally, [6] seems to be the only work containing convergence-rate results for *Shapley-effect* estimators.

To the best of our knowledge, this article is the first to provide an estimator of a function's Shapley effects that is computationally tractable for a moderate-to-large number of inputs and function evaluations. This article is also the first to establish posterior contraction rates for a *Bayesian* estimator of a function's Sobol' indices and Shapley effects. Our approach is a metamodel-based one, and the metamodel we use is Bayesian Additive Regression Trees (BART) [26] which is an increasingly popular tool for complex regression problems and as emulators of expensive computer simulations [27, 28, 29]. BART is a nonparametric sum-of-trees model embedded in a Bayesian inferential framework. Unlike many other metamodels, BART can easily incorporate categorical inputs, avoids strong parametric assumptions, and is relatively quick to fit even on a large number of observations. In particular, fitting a BART model does not perform the  $O(n^3)$  matrix decompositions required for a GP to fit to  $n$  data points. BART even has been shown to be resilient to the inclusion of inert inputs, particularly when the BART prior incorporates either the sparsity-inducing Dirichlet prior of [30] or the spike-and-tree prior of [31, 32]. Furthermore, the Bayesian framework provides natural uncertainty quantification for both predictions and sensitivity-index estimates. Per the review article of [33], the work in this article can be considered part of the "cross-fertilization of ideas between [machine learning] and [sensitivity analysis]."

The computation of our estimators relies on a particular feature of BART, namely that the sum-of-trees model assumption implies every realization of a BART random function is piecewise constant. [34] uses this to establish closed-form expressions for Sobol' index estimates

computed using a fitted BART model (such estimates will be denoted as “BART-based Sobol’ indices” for the rest of this article) that are easy to compute after the BART model is fit. Section 2 will show these closed-form expressions can be used to compute BART-based Shapley effects, but because the number of expressions to compute increases dramatically, Section 4 discusses computationally friendly approximations. On the other hand, our contraction-rate results rely heavily on recent BART theory from [35], who introduce the large class of sparse piecewise heterogeneous anisotropic Hölder functions and show that over this function class, the contraction rate for Bayesian forests is optimal up to a logarithmic factor.

This article is organized as follows. Section 2 reviews BART, piecewise heterogeneous anisotropic functions, posterior contraction, Sobol’ indices, and Shapley effects. Section 3 provides posterior contraction results for BART-based Sobol’ indices and Shapley effects. Section 4 discusses the computation of BART-based Shapley effects and Section 5 showcases their performance on numerical examples (the analogous discussion for BART-based Sobol’ indices can be found in [34]). Section 6 provides discussion on future work.

**1.1. Notation.** For any positive integer  $m$ , denote  $[m] := \{1, \dots, m\}$ . We also make the distinction that  $\subset$  denotes a proper subset whereas  $\subseteq$  denotes any subset. Let  $L^2 \equiv L^2([0, 1]^p)$  denote the space of real-valued, square-integrable functions on the unit hypercube  $[0, 1]^p$ . Finally, let  $\mathbb{E}$  and  $\mathbb{V}$  respectively denote the expectation and variance operator.

**2. Review.** Mirroring [35], this article considers regression settings with either a fixed or random design. The regression model with *fixed* design is

$$(2.1) \quad Y_i = f_0(\mathbf{x}_i) + \varepsilon_i, \quad \varepsilon_i \sim N(0, \sigma_0^2), \quad i = 1, \dots, n,$$

where  $\sigma_0^2 < \infty$  and each covariate  $\mathbf{x}_i \in [0, 1]^p$  is fixed. A fixed design would be assumed if for example the trees in BART are allowed to split only on observed covariate values (which was a specification used in the seminal BART paper [36]) or on dyadic midpoints of the domain. The regression model with *random* design is

$$(2.2) \quad Y_i = f_0(\mathbf{X}_i) + \varepsilon_i, \quad \mathbf{X}_i \sim \pi, \quad \varepsilon_i \sim N(0, \sigma_0^2), \quad i = 1, \dots, n,$$

where  $\sigma_0^2 < \infty$ , each  $\mathbf{X}_i \in [0, 1]^p$  is a  $p$ -dimensional random covariate, and  $\pi$  is a probability measure such that  $\text{supp}(\pi) \subseteq [0, 1]^p$ . A random design would be assumed for estimation problems such as density estimation or regression/classification with random design. Our results in Section 3 deal separately with fixed or random designs.

**2.1. BART.** In a regression setting in the form of either (2.1) and (2.2), a BART model approximates the unknown function  $f_0$  by a sum of  $T$  regression trees:

$$(2.3) \quad f_0(\cdot) \approx \sum_{t=1}^T g(\cdot; \Theta_t),$$

where each regression-tree function  $g(\cdot; \Theta_t) : [0, 1]^p \rightarrow \mathbb{R}$  is piecewise constant over the input space, which implies the sum on the right hand side of (2.3) is also piecewise constant. For each  $t$ , the parameter set  $\Theta_t$  determines a partition of the input space and the values assigned to each partitioned piece of the input space. Each tree induces a partition by recursively

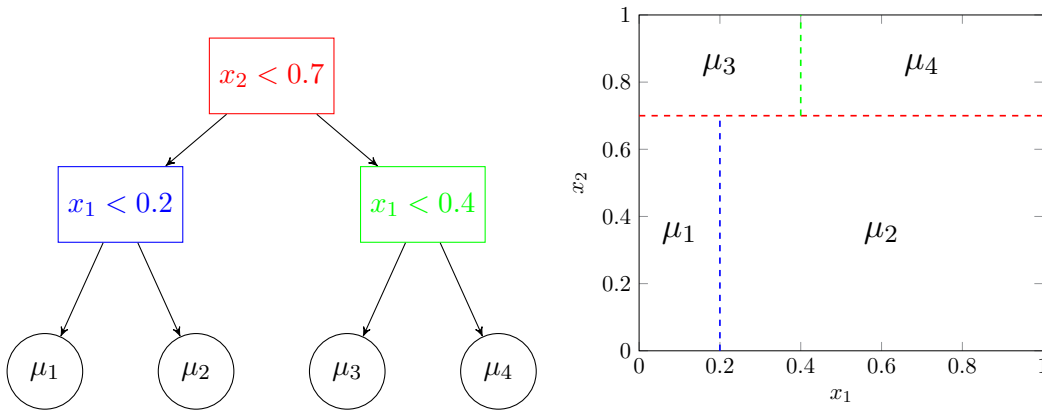


Figure 1: An example tree shown graphically (left) and as a piecewise-constant regression function (right) on the input space  $[0, 1]^2$ .

applying binary splitting rules to split the domain  $[0, 1]^p$  into boxes (i.e. hyperrectangles); Figure 1 shows an illustrative example. To regularize the model fit, the BART prior over the parameters  $\{\Theta_t\}_{t=1}^T$  keeps the individual tree effects small, which causes each function  $g(\cdot; \Theta_t)$  to contribute a small portion to the total approximation of  $f_0$ . The expected response  $\mathbb{E}[Y(\mathbf{x}) \mid \{\Theta_t\}_{t=1}^T]$  at a given input  $\mathbf{x}$  is then the sum of each of the contributions  $g(\mathbf{x}; \Theta_t)$ .

Though the right hand side of (2.3) is piecewise constant, [35] shows that BART can, under certain conditions, approximate the unknown function  $f_0$  (which itself need not be piecewise constant) arbitrarily closely with attractive posterior contraction rates. After reviewing the concept of contraction rates, we state for convenience the conditions made in the theorems of [35] that our contraction-rate results rely on. Because these conditions are not the focus of this paper, we leave discussion of the context behind these conditions to [35].

**2.1.1. Posterior contraction.** A posterior contraction rate quantifies how quickly a posterior distribution approaches the true parameter of the data's distribution. We use a simplified version of the definition from [37]: for every  $n \in \mathbb{N}$ , let  $X^{(n)}$  be an observation in a sample space  $(\mathcal{X}^{(n)}, \mathcal{X}^{(n)})$  with distribution  $P_{\theta}^{(n)}$  indexed by  $\theta$  belonging to a first countable topological space  $\Theta$ . Given a prior  $\Pi_n$  on the Borel sets of  $\Theta$ , let  $\Pi_n(\cdot \mid X^{(n)})$  be (a fixed particular version of) the posterior distribution.

**Definition 2.1 (Posterior contraction rate).** A sequence  $\{\varepsilon_n\}_{n \in \mathbb{N}}$  is a posterior contraction rate at the parameter  $\theta_0$  with respect to the semimetric  $d$  if  $\Pi_n(\theta : d(\theta, \theta_0) \geq M_n \varepsilon_n \mid X^{(n)}) \rightarrow 0$  in  $P_{\theta_0}^{(n)}$ -probability, for every  $M_n \rightarrow \infty$ .

Note that if there exists a constant  $M > 0$  such that  $\Pi_n(\theta : d(\theta, \theta_0) \geq M \varepsilon_n \mid X^{(n)}) \rightarrow 0$  in  $P_{\theta_0}^{(n)}$ -probability, then the sequence  $\{\varepsilon_n\}_{n \in \mathbb{N}}$  satisfies the definition of posterior contraction rate. This will be relevant in interpreting Corollaries 3.3 and 3.5 in Section 3.

**2.1.2. Piecewise heterogeneous anisotropic functions.** Next we introduce the aforementioned conditions of the theorems of [35] relevant to our work. The first set of conditions

involves what values of  $f_0$  and  $\sigma_0^2$  are allowed for BART to contract around  $f_0$ . A common assumption for  $f_0$  is isotropic smoothness, but this excludes the realistic scenario that  $f_0$  is discontinuous and has different degrees of smoothness in different directions and regions. [35] introduce a new class of *piecewise heterogeneous anisotropic* functions whose domain is partitioned into many boxes (i.e. hyperrectangles), each of which has its own anisotropic smoothness with the same harmonic mean. First assume  $f_0$  is  $d$ -sparse, i.e. there exists a function  $h_0 : [0, 1]^d \rightarrow \mathbb{R}$  and a subset  $S_0 \subseteq [p]$  with  $|S_0| = d$  such that  $f_0(\mathbf{x}) = h_0(\mathbf{x}_{S_0})$  for any  $\mathbf{x} \in [0, 1]^p$ . For any given box  $\Xi \subseteq [0, 1]^d$ , smoothness parameter  $\boldsymbol{\alpha} = (\alpha_1, \dots, \alpha_d)^T \in (0, 1]^d$ , and Hölder coefficient  $\lambda < \infty$ , an *anisotropic  $\boldsymbol{\alpha}$ -Hölder space* on  $\Xi$  is defined as

$$\mathcal{H}_\lambda^{\boldsymbol{\alpha}, d}(\Xi) := \left\{ h : \Xi \rightarrow \mathbb{R}; |h(x) - h(y)| \leq \lambda \sum_{j=1}^d |x_j - y_j|^{\alpha_j}, x, y \in \Xi \right\}.$$

Though  $h_0$  might have different anisotropic smoothness on different boxes, an important assumption to make is that all boxes have the same harmonic mean. Thus define the set  $\mathcal{A}_{\bar{\alpha}}^{R, d}$  to be the set of  $R$ -tuples of smoothness parameters that have harmonic mean  $\bar{\alpha} \in (0, 1]$ :

$$\mathcal{A}_{\bar{\alpha}}^{R, d} := \left\{ (\boldsymbol{\alpha}_1, \dots, \boldsymbol{\alpha}_R) : \boldsymbol{\alpha}_r \in (0, 1]^d, \bar{\alpha}^{-1} = p^{-1} \sum_{j=1}^d \alpha_{rj}^{-1}, r \in [R] \right\}.$$

Given a box partition  $(\Xi_1, \dots, \Xi_R)$  of  $[0, 1]^d$  with boxes  $\Xi_r \subseteq [0, 1]^d$  and a smoothness  $R$ -tuple  $A_{\bar{\alpha}} \in \mathcal{A}_{\bar{\alpha}}^{R, d}$  for some  $\bar{\alpha} \in (0, 1]$ , define a *piecewise heterogeneous anisotropic Hölder space* as

$$\mathcal{H}_\lambda^{A_{\bar{\alpha}}, d}(\mathfrak{X}) := \left\{ h : [0, 1]^d \rightarrow \mathbb{R}; h|_{\Xi_r} \in \mathcal{H}_\lambda^{\boldsymbol{\alpha}_r, d}(\Xi_r), r \in [R] \right\}.$$

To extend a function from a sparse domain to the original domain  $[0, 1]^p$ , for any nonempty subset  $S \subseteq [p]$  define  $W_S^p : \mathcal{C}(\mathbb{R}^{|S|}) \rightarrow \mathcal{C}(\mathbb{R}^p)$  as the map that extends  $h \in \mathcal{C}(\mathbb{R}^{|S|})$  to the function  $W_S^p h : \mathbf{x} \rightarrow h(\mathbf{x}_S)$  where  $\mathbf{x} \in [0, 1]^p$ . With this definition, the space  $\mathcal{H}_\lambda^{A_{\bar{\alpha}}, d}(\mathfrak{X})$  from the preceding panel can be extended to the corresponding  *$d$ -sparse piecewise heterogeneous anisotropic Hölder space*

$$\Gamma_\lambda^{A_{\bar{\alpha}}, d, p}(\mathfrak{X}) := \bigcup_{S \subseteq [p]: |S|=d} W_S^p \left( \mathcal{H}_\lambda^{A_{\bar{\alpha}}, d}(\mathfrak{X}) \right).$$

With these definitions, we can now state the required assumptions on the true parameters  $f_0$  and  $\sigma^2$ .

- (A1) For  $d > 0$ ,  $\lambda > 0$ ,  $R > 0$ ,  $\mathfrak{X} = (\Xi_1, \dots, \Xi_R)$ , and  $A_{\bar{\alpha}} \in \mathcal{A}_{\bar{\alpha}}^{R, d}$  with  $\bar{\alpha} \in (0, 1]$ , the true function satisfies  $f_0 \in \Gamma_\lambda^{A_{\bar{\alpha}}, d, p}(\mathfrak{X})$  or  $f_0 \in \Gamma_\lambda^{A_{\bar{\alpha}}, d, p}(\mathfrak{X}) \cap \mathcal{C}([0, 1]^p)$ .
- (A2) It is assumed that  $d, p, \lambda, R$ , and  $\bar{\alpha}$  satisfy  $\epsilon_n \ll 1$ , where

$$(2.4) \quad \epsilon_n := \sqrt{\frac{d \log p}{n}} + (\lambda d)^{d/(2\bar{\alpha}+d)} \left( \frac{R \log n}{n} \right)^{\bar{\alpha}/(2\bar{\alpha}+d)}.$$

- (A3) The true function  $f_0$  satisfies  $\|f_0\|_\infty \lesssim \sqrt{\log n}$ .
- (A4) The true variance parameter satisfies  $\sigma^2 \in [C_0^{-1}, C_0]$  for some sufficiently large  $C_0 > 1$ .

**2.1.3. Split-net.** The second set of conditions (of the theorems of [35] relevant to our work) involves the split values  $c$  allowed in the binary split rules “ $x_j < c$ ” of the regression trees (again, see Figure 1 for an illustration). If a partition of  $[0, 1]^p$  can be created using the aforementioned tree-based procedure, call it a *flexible tree partition*. To restrict a flexible tree partition by a set of allowable split values in the binary split rules, for any integer  $b_n$  define a *split-net*  $\mathcal{Z}$  to be a finite set of points in  $[0, 1]^p$  at which possible splits occur along coordinates. That is, the allowable split values for any input dimension  $j \in [p]$  are the  $j$ th components of the points in the split-net. For a given split-net  $\mathcal{Z}$ , a flexible tree partition  $(\Omega_1, \dots, \Omega_K)$  of  $[0, 1]^p$  with boxes  $\Omega_k \subseteq [0, 1]^p$ ,  $k \in [K]$ , is called a  $\mathcal{Z}$ -*tree partition* if every split occurs at points in  $\mathcal{Z}$ .

A split net should be dense enough for a resulting partition to be close enough to the underlying partition  $\mathfrak{X}^* = (\Xi_1^*, \dots, \Xi_R^*)$  of the true function  $f_0$ . For any two box partitions  $\mathfrak{Y}^1 = (\Psi_1^1, \dots, \Psi_J^1)$  and  $\mathfrak{Y}^2 = (\Psi_1^2, \dots, \Psi_J^2)$  with the same number  $J$  of boxes, their closeness will be measured using the Hausdorff-type divergence

$$\Upsilon(\mathfrak{Y}^1, \mathfrak{Y}^2) := \min_{\tau \in \text{Perm}[J]} \max_{r \in [J]} \text{Haus}(\Psi_r^1, \Psi_{\tau(r)}^2)$$

where  $\text{Perm}[J]$  denotes the set of all permutations of  $[J]$  and  $\text{Haus}(\cdot, \cdot)$  is the Hausdorff distance. For a subset  $S \subseteq [p]$ , a box partition of  $[0, 1]^p$  is called  $S$ -*chopped* if every box  $\Psi$  in the box partition satisfies  $\max_{j \in S} \text{len}([\Psi]_j) < 1$  and  $\min_{j \notin S} \text{len}([\Psi]_j) = 1$ . For a given subset  $S \subseteq [p]$ , consider an  $S$ -chopped partition  $\mathfrak{Y}$  of  $[0, 1]^p$  with  $J$  boxes. For any given  $c_n \geq 0$ , a split-net  $\mathcal{Z}_n$  is said to be  $(\mathfrak{Y}, c_n)$ -*dense* if there exists an  $S$ -chopped  $\mathcal{Z}_n$ -tree partition  $\mathcal{T}_n$  of  $[0, 1]^p$  with  $J$  boxes such that  $\Upsilon(\mathfrak{Y}, \mathcal{T}_n) \leq c_n$ .

A split net should also be regular enough (defined below) for a tree partition to capture local features of  $f_0$  on each box. Assume the underlying partition  $\mathfrak{X}^*$  can be approximated well by an  $S(\mathfrak{X}^*)$ -chopped  $\mathcal{Z}$ -tree partition  $(\Omega_1^*, \dots, \Omega_R^*) := \arg \min_{\mathcal{T} \in \mathcal{T}_{S(\mathfrak{X}^*), R, \mathcal{Z}}} \Upsilon(\mathfrak{X}^*, \mathcal{T})$ . In each box  $\Omega_r^*$ , the idea is to allow splits to occur more often along the input dimensions with less smoothness. Given a split-net  $\mathcal{Z}$  and splitting coordinate  $j$ , define the *midpoint-split* of a box  $\Psi$  as the bisection of  $\Psi$  along coordinate  $j$  at the  $\lceil \tilde{b}_j(\mathcal{Z}, \Psi)/2 \rceil$ th split-candidate in  $[\mathcal{Z}]_j \cap \text{int}([\Psi]_j)$ , where  $\tilde{b}_j(\mathcal{Z}, \Psi)$  is the cardinality of  $[\mathcal{Z}]_j \cap \text{int}([\Psi]_j)$ . Given a smoothness vector  $\alpha \in (0, 1]^d$ , box  $\Psi \subseteq [0, 1]^p$ , split-net  $\mathcal{Z}$ , integer  $L > 0$ , and index set  $S = \{s_1, \dots, s_d\} \subseteq [p]$ , define the *anisotropic  $k$ -d tree AKD*  $\text{AKD}(\Psi; \mathcal{Z}, \alpha, L, S)$  as the iterative splitting procedure that partitions  $\Psi$  into disjoint boxes  $\Omega_1^\circ, \dots, \Omega_{2^{L^\circ}}^\circ$  as follows:

1. Set  $\Omega_1^\circ = \Psi$  and set counter  $l_j = 0$  for each  $j \in [d]$ .
2. Let  $L^\circ = \sum_{j=1}^d l_j$  for the current counters. For splits at iteration  $1 + L^\circ$ , choose  $j' = \min\{\arg \min_j l_j \alpha_j\}$ . Midpoint-split all boxes  $\Omega_1^\circ, \dots, \Omega_{2^{L^\circ}}^\circ$  with the given  $\mathcal{Z}$  and splitting coordinate  $s_{j'}$ . Relabel the generated new boxes as  $\Omega_1^\circ, \dots, \Omega_{2^{1+L^\circ}}^\circ$ , and then increment  $l_{j'}$  by one.
3. Repeat step 2 until either the updated  $L^\circ$  equals  $L$  or the midpoint-split is no longer available. Return counters  $l_1, \dots, l_d$  and boxes  $\Omega_1^\circ, \dots, \Omega_{2^{L^\circ}}^\circ$ .

For a given box  $\Psi \subseteq [0, 1]^p$ , smoothness vector  $\alpha \in (0, 1]^d$ , integer  $L > 0$ , and index set  $S = \{s_1, \dots, s_d\} \subseteq [p]$ , a split-net  $\mathcal{Z}$  is called  $(\Psi, \alpha, L, S)$ -*regular* if the counters and boxes returned by  $\text{AKD}(\Psi; \mathcal{Z}, \alpha, L, S)$  satisfy  $L^\circ = L$  and  $\max_k \text{len}([\Omega_k^\circ]_{s_j}) \lesssim \text{len}([\Psi]_{s_j}) 2^{-l_j}$  for every  $j \in [d]$ .

With these definitions, we can now state the needed assumptions on the sequence  $\{\mathcal{Z}_n\}_{n=1}^\infty$  of split-nets.

- (A5) Each split-net  $\mathcal{Z}_n$  satisfies  $\max_{1 \leq j \leq p} \log b_j(\mathcal{Z}_n) \lesssim \log n$ , where  $b_j(\mathcal{Z}_n)$  is the cardinality of the set  $\{z_j : (z_1, \dots, z_p) \in \mathcal{Z}_n\}$ .
- (A6) Each split-net  $\mathcal{Z}_n$  is suitably dense and regular to construct a  $\mathcal{Z}_n$ -tree partition  $\hat{\mathcal{T}}$  such that there exists a simple function  $\hat{f}_0 \in \mathcal{F}_{\hat{\mathcal{T}}}$  satisfying  $\|f_0 - \hat{f}_0\|_n \lesssim \bar{\epsilon}_n$ , where

$$(2.5) \quad \bar{\epsilon}_n := (\lambda d)^{d/(2\bar{\alpha}+d)} ((R \log n)/n)^{\bar{\alpha}/(2\bar{\alpha}+d)},$$

the empirical  $L_2$ -norm  $\|\cdot\|_n$  is defined as  $\|f\|_n^2 = n^{-1} \sum_{i=1}^n |f(\mathbf{x}_i)|^2$ , and  $\mathcal{F}_{\hat{\mathcal{T}}}$  is the set of functions on  $[0, 1]^p$  that are constant on each piece of the partition  $\hat{\mathcal{T}}$ .

- (A7) Each  $\mathcal{Z}_n$ -tree partition  $(\Omega_1^*, \dots, \Omega_R^*)$  approximating the underlying partition  $\mathfrak{X}^*$  for the true function  $f_0$  satisfies  $\max_{r \in [R]} \text{depth}(\Omega_r^*) \lesssim \log n$ , where  $\text{depth}$  means the depth of a node (i.e. the number of nodes along the path from the root node down to that node).

Finally, we state the required prior specification.

- (P1) Each tree partition in the ensemble is independently assigned a tree prior with Dirichlet sparsity from [30]. This sparse Dirichlet prior places Dirichlet prior on the proportion vector used to select the splitting coordinate  $j$  during the creation of a split rule.
- (P2) The step-heights of the regression-tree functions are each assigned a normal prior with a zero-mean and a covariance matrix whose eigenvalues are bounded below and above.
- (P3) The variance parameter  $\sigma^2$  for the regression model is assigned an inverse gamma prior.

[35] make the above assumptions and prior specification for their contraction-rate results in the fixed design setting (2.1). For their contraction-rate results in the random design setting (2.2), a few of the above assumptions and prior specifications are replaced by the following:

- (A3\*) The true function  $f_0$  satisfies  $\|f_0\|_\infty \leq C_0^*$  for some sufficiently large  $C_0^* > 0$ .
- (A6\*) The split-net  $\mathcal{Z}$  is suitably dense and regular to construct a  $\mathcal{Z}$ -tree partition  $\hat{\mathcal{T}}$  such that there exists  $\hat{f}_0 \in \mathcal{F}_{\hat{\mathcal{T}}}$  satisfying  $\|f_0 - \hat{f}_0\| \lesssim \bar{\epsilon}_n$  where  $\bar{\epsilon}_n$  is given by (2.5).
- (P2\*) A prior on the compact support  $[-\bar{C}_1, \bar{C}_1]$  is assigned to the step-heights of the regression-tree functions for some  $\bar{C}_1 > C_0^*$ .
- (P3\*) A prior on the compact support  $[\bar{C}_2^{-1}, \bar{C}_2]$  is assigned to the variance parameter  $\sigma^2$  for some  $\bar{C}_2 > C_0$ .

**2.2. Sobol' indices.** [1, 38] shows that if the random variable  $\mathbf{X}$  follows an orthogonal distribution whose support is  $[0, 1]^p$  and if  $f \in L^2$ , then the variance of  $f(\mathbf{X})$  can be decomposed into a sum of terms attributed to single inputs or to interactions between sets of inputs:

$$(2.6) \quad \mathbb{V}f(\mathbf{X}) = \sum_{j=1}^p V_j + \sum_{j=1}^p \sum_{k < j} V_{jk} + \dots + V_{1,2,\dots,p}$$

where we recursively define for each variable index set  $P \subseteq [p]$

$$V_P := \mathbb{V}(\mathbb{E}[f(\mathbf{X}) \mid \mathbf{X}_P]) - \sum_{Q \subset P} V_Q$$

where we set  $V_\emptyset = 0$  and the relation  $\subset$  denotes a strict subset. For any variable index  $j \in [p]$ , the term  $V_{\{j\}} = V_j$  is known as the  $j$ th (unnormalized) first-order (or main-effect) Sobol' index, and the sum  $T_j = \sum_{P \subseteq ([p] \setminus \{j\})} V_{P \cup \{j\}}$  is known as the  $j$ th (unnormalized) total-effect Sobol' index. We note that  $T_j \geq V_j \geq 0$  for all  $j \in [p]$ .

The  $V_P$  terms in (2.6) are often divided by the total variance to produce the normalized terms  $V_P / [\mathbb{V}f(\mathbf{X})]$ , which have the nice interpretation of being the proportion of the total variance attributed to the interaction between the variables whose indices are in the index set  $P$ . If  $P$  is the singleton  $\{j\}$ , then the normalized term  $V_j / [\mathbb{V}f(\mathbf{X})]$  can be interpreted as the proportion of the total variance attributed to variable  $j$  by itself. Despite this nice interpretation, the remainder of the article will assume that such indices are unnormalized unless otherwise stated.

To see why these indices' interpretation requires  $\mathbf{X}$  to follow an orthogonal distribution, we extend the definition of  $V_P$  by removing the orthogonality assumption. That is, we allow  $\mathbf{X}$  to follow a possibly non-orthogonal distribution  $\pi$  whose support is  $[0, 1]^p$ . We first define the functional  $c_{P,\pi} : L^2 \rightarrow \mathbb{R}$  as

$$(2.7) \quad c_{P,\pi}(f) = \mathbb{V}_\pi(\mathbb{E}_\pi[f(\mathbf{X}) \mid \mathbf{X}_P]) = \mathbb{E}_\pi[(\mathbb{E}_\pi[f(\mathbf{X}) \mid \mathbf{X}_P])^2] - [\mathbb{E}_\pi f(\mathbf{X})]^2$$

for any  $f \in L^2$ . Then the generalized  $V_P$  under the distribution  $\pi$  is recursively defined as

$$V_{P,\pi}(f) := c_{P,\pi}(f) - \sum_{Q \subset P} V_{Q,\pi}(f),$$

where again we set  $V_{\emptyset,\pi}(f) = 0$ . Similarly, we define the generalized  $j$ th total-effect term as

$$T_{j,\pi}(f) = \sum_{P \subseteq ([p] \setminus \{j\})} V_{P \cup \{j\},\pi}(f)$$

where the binary relation  $\subseteq$  denotes a subset that is not necessarily strict. Recall that if  $\pi$  is orthogonal and  $f \in L^2$ , then  $T_{j,\pi}(f) \geq V_{j,\pi}(f) \geq 0$  for all  $j \in [p]$  and the variance decomposition (2.6) (where orthogonality implies  $V_P = V_{P,\pi}(f)$  for all  $P \subseteq [p]$ ) holds. However, Theorem 2 of [2] asserts the existence of a non-orthogonal distribution  $\pi$  and a function  $f \in L^2$  such that  $\sum_{j=1}^p V_{j,\pi}(f) > \mathbb{V}_\pi f(\mathbf{X}) > \sum_{j=1}^p T_{j,\pi}(f)$ . In such a case, these Sobol' indices can no longer be interpreted as in the orthogonal case.

**2.3. Shapley effects.** One way to measure variable activity that can be used regardless of dependence among inputs are the Shapley effects defined by [2] as the Shapley values in [4] using the functional (2.7) as the ‘‘value’’ or ‘‘cost.’’ For  $j \in [p]$  the  $j$ th Shapley effect is defined as

$$(2.8) \quad S_{j,\pi}(f) = (p!)^{-1} \sum_{P \subseteq ([p] \setminus \{j\})} (p - |P| - 1)! |P|! [c_{P \cup \{j\},\pi}(f) - c_{P,\pi}(f)],$$

which has the desirable property

$$\sum_{j=1}^p S_{j,\pi}(f) = \mathbb{V}_\pi f(\mathbf{X})$$



for any distribution  $\pi$  whose support is  $[0, 1]^p$ , *regardless of whether  $\pi$  is orthogonal*. Hence, the  $j$ th Shapley effect (after normalization) can be nicely interpreted as the contribution of input  $j$  to the total output variance. Furthermore, if  $\pi$  is orthogonal, then

$$(2.9) \quad V_{j,\pi}(f) \leq S_{j,\pi}(f) \leq T_{j,\pi}(f)$$

for any  $f \in L^2$  and  $j \in [p]$  [4, Section 3], i.e. the  $j$ th Shapley effect is bounded between the  $j$ th main-effect Sobol' index and the  $j$ th total-effect Sobol' index.

The astute reader will note the calculation of (2.8) can be prohibitively costly due to it being a sum of values (2.7) over all subsets of a set  $[p] \setminus \{j\}$  which has  $p - 1$  elements. Its computational tractability will be discussed in Section 4.

**3. Main results.** The aim of this section is to establish Corollaries 3.3 and 3.5, which are our contraction-rate results for estimators of Sobol' indices and Shapley effects under either the fixed design (2.1) or the random design (2.2). Our proofs of these corollaries rely on these sensitivity indices having a property similar to but slightly less restrictive than Lipschitz continuity (this property is defined Lemma 3.1 below). However, the tasks of proving this property for all of these sensitivity indices are somewhat tedious and very similar to each other. If we note that these indices are linear combinations of the functional  $c_{P,\pi}$  defined in (2.7), we can use Lemma 3.1 below to reduce the above tasks to the single task of proving this property for  $c_{P,\pi}$ .

**Lemma 3.1.** *Suppose the following relationship holds true for all indices  $k$  in a finite set  $\mathcal{A}$ : given two metric spaces  $(X, d_X)$  and  $(X_0, d_X)$  that share the same metric, there exists a real constant  $C > 0$  such that, for all  $(x, x_0) \in X \times X_0$ , the function  $\phi_k : X \cup X_0 \rightarrow \mathbb{R}$  satisfies*

$$|\phi_k(x) - \phi_k(x_0)| \leq C d_X(x, x_0).$$

Then any set  $\{a_k\}_{k \in \mathcal{A}}$  of real numbers satisfies

$$\left| \sum_{k \in \mathcal{A}} a_k \phi_k(x) - \sum_{k \in \mathcal{A}} a_k \phi_k(x_0) \right| \leq C^* d_X(x, x_0).$$

where  $C^* = C \sum_{k \in \mathcal{A}} |a_k|$ .

*Proof of Lemma 3.1.* The LHS of the inequality we wish to prove is bounded above by

$$\sum_{k \in \mathcal{A}} |a_k| |\phi_k(x) - \phi_k(x_0)| \leq \sum_{k \in \mathcal{A}} |a_k| C d_X(x, x_0)$$

where the RHS of the above inequality is exactly  $C^* d_X(x, x_0)$ . ■

**3.1. Nonparametric regression with random design.** This section assumes the random-design regression setting (2.2); all expectations in this section are with respect to the probability measure  $\pi$  in (2.2).

**Theorem 3.2.** *Assume  $(A\mathfrak{B}^*)$ . If  $f \in L^2([0, 1]^p)$  shares the same bound  $C_0^*$  from  $(A\mathfrak{B}^*)$ , then for any subset  $P \subseteq [p]$  and distribution  $\pi$  with support  $[0, 1]^p$  we have*

$$|c_{P,\pi}(f) - c_{P,\pi}(f_0)| \leq 4C_0^* \|f - f_0\|_{2,\pi}$$

for the functional  $c_{P,\pi}$  defined in (2.7).

*Proof.* Note that

$$\begin{aligned} |c_{P,\pi}(f) - c_{P,\pi}(f_0)| &= \left| \left( \mathbb{E}[(\mathbb{E}[f(\mathbf{X}) | \mathbf{X}_P])^2 - (\mathbb{E}[f_0(\mathbf{X}) | \mathbf{X}_P])^2] \right) - \left( \mathbb{E}[f(\mathbf{X})]^2 - \mathbb{E}[f_0(\mathbf{X})]^2 \right) \right| \\ &\leq \mathbb{E} \left| (\mathbb{E}[f(\mathbf{X}) | \mathbf{X}_P])^2 - (\mathbb{E}[f_0(\mathbf{X}) | \mathbf{X}_P])^2 \right| + \left| \mathbb{E}[f(\mathbf{X})]^2 - \mathbb{E}[f_0(\mathbf{X})]^2 \right|. \end{aligned}$$

From the assumption that  $f$  and  $f_0$  are bounded in supremum norm by  $C_0^*$ , we get

$$\begin{aligned} \left| \mathbb{E}[f(\mathbf{X})]^2 - \mathbb{E}[f_0(\mathbf{X})]^2 \right| &= \left| \mathbb{E}[f(\mathbf{X}) + f_0(\mathbf{X})][f(\mathbf{X}) - f_0(\mathbf{X})] \right| \\ &\leq 2C_0^* \mathbb{E}|f(\mathbf{X}) - f_0(\mathbf{X})|. \end{aligned}$$

We can similarly deduce for any  $\mathbf{X}_P$  that

$$\left| (\mathbb{E}[f(\mathbf{X}) | \mathbf{X}_P])^2 - (\mathbb{E}[f_0(\mathbf{X}) | \mathbf{X}_P])^2 \right| \leq 2C_0^* \mathbb{E}|f(\mathbf{X}) - f_0(\mathbf{X}) | \mathbf{X}_P|.$$

Then

$$\begin{aligned} |c_{P,\pi}(f) - c_{P,\pi}(f_0)| &\leq \mathbb{E}[2C_0^* \mathbb{E}|f(\mathbf{X}) - f_0(\mathbf{X}) | \mathbf{X}_P|] + 2C_0^* \mathbb{E}|f(\mathbf{X}) - f_0(\mathbf{X})| \\ &= 4C_0^* \mathbb{E}|f(\mathbf{X}) - f_0(\mathbf{X})|. \end{aligned}$$

To finish, Jensen's inequality implies  $\mathbb{E}|f(\mathbf{X}) - f_0(\mathbf{X})| \leq \|f - f_0\|_{2,\pi}$ . ■

**Corollary 3.3.** *Under the assumptions of Theorem 4 of [35] – Assumptions (A1), (A2), (A3\*), (A4), (A5), (A6\*), and (A7), and the prior assigned through (P1), (P2\*), and (P3\*) – and Theorem 3.2 above, there exist positive constants  $L_1$ ,  $L_2$ , and  $L_3$  such that*

$$\begin{aligned} \mathbb{E}_0 \Pi \left\{ (f, \sigma^2) : |V_{P,\pi}(f) - V_{P,\pi}(f_0)| + |\sigma^2 - \sigma_0^2| > L_1 \epsilon_n \mid Y_1, \dots, Y_n \right\} &\rightarrow 0, \\ \mathbb{E}_0 \Pi \left\{ (f, \sigma^2) : |T_{j,\pi}(f) - T_{j,\pi}(f_0)| + |\sigma^2 - \sigma_0^2| > L_2 \epsilon_n \mid Y_1, \dots, Y_n \right\} &\rightarrow 0, \\ \text{and } \mathbb{E}_0 \Pi \left\{ (f, \sigma^2) : |S_{j,\pi}(f) - S_{j,\pi}(f_0)| + |\sigma^2 - \sigma_0^2| > L_3 \epsilon_n \mid Y_1, \dots, Y_n \right\} &\rightarrow 0 \end{aligned}$$

for  $\epsilon_n$  in (2.4).

*Proof.* Below is the proof just for the  $j$ th (where  $j \in [p]$ ) total-effect Sobol' index. The same argument can be followed to obtain the corresponding results for any main-effect Sobol' index and any Shapley effect after making the appropriate substitutions for the  $a_P$  below. Lemma 3.1 and Theorem 3.2 together imply

$$|T_{j,\pi}(f) - T_{j,\pi}(f_0)| \leq D_2 \|f - f_0\|_{2,\pi}.$$

where the constant  $D_2 := \max\{1, 4C_0^* \sum_{P \in [p]} |a_P|\}$  and the real values  $a_P$  are the coefficients corresponding to  $T_{j,\pi}$  expressed as a linear combination of  $c_{P,\pi}$ . For any constant  $\delta > 0$ , define the two sets

$$\begin{aligned} A_\delta &:= \{(f, \sigma^2) : |T_{j,\pi}(f) - T_{j,\pi}(f_0)| + |\sigma^2 - \sigma_0^2| > \delta\} \\ B_\delta &:= \{(f, \sigma^2) : D_2 |T_{j,\pi}(f) - T_{j,\pi}(f_0)| + D_2 |\sigma^2 - \sigma_0^2| > \delta\}. \end{aligned}$$

Because  $D_2 \geq 1$ , we have  $A_\delta \subseteq B_\delta$  for all  $\delta > 0$ . Let  $\mathcal{D}_n := \{(X_1, Y_1), \dots, (X_n, Y_n)\}$ . By Theorem 4 of [35], there exists a constant  $M > 0$  such that  $\mathbb{E}_0 \Pi(B_{L_2 \epsilon_n} \mid \mathcal{D}_n) \rightarrow 0$ , where  $L_2 = D_2 M$ . Because  $A_{L_2 \epsilon_n} \subseteq B_{L_2 \epsilon_n}$  for all  $n$ , we have  $\mathbb{E}_0 \Pi(A_{L_2 \epsilon_n} \mid \mathcal{D}_n) \rightarrow 0$ . ■

Regarding the constant  $D_2$  in the proof, the sum  $\sum_{P \in [p]} |a_P|$  grows exponentially in  $p$ . But if  $p$  is large, it is typically assumed the underlying regression function  $f_0$  can be written as a function of a subset  $S_0 \subset [p]$  of  $d \ll p$  variables, which would associate  $a_P$  with a zero value of  $c_{P,\pi}(f_0)$  if  $P$  has any indices not in  $S_0$ . Furthermore, because each tree in a BART regression function  $f$  will also typically be a function of at most  $d$  variables, this sparsity assumption would also associate  $a_P$  with a zero value of  $c_{P,\pi}(f)$  if  $P$  has any indices not in  $S_0$ . If  $a_P$  is associated with a zero value of both  $c_{P,\pi}(f_0)$  and  $c_{P,\pi}(f)$ , it can be omitted from the upper bound of Lemma 3.1. Thus if  $a_P$  can be omitted from the upper bound for all  $P$  with indices outside of  $S_0$ , what remains is a sum of  $O(2^d) \ll O(2^p)$  terms.

**3.2. Nonparametric regression with fixed design.** This section assumes the fixed-design regression setting (2.1); all expectations in this section are with respect to the probability measure  $P_{\mathcal{X}}(\cdot) = n^{-1} \sum_{\mathbf{x} \in \mathcal{X}} \delta_{\mathbf{x}}(\cdot)$  where  $\mathcal{X}$  is the set of the fixed covariates assumed in (2.1).

**Theorem 3.4.** *Assume (A3). If  $f \in L^2([0, 1]^p)$  shares the same bound  $\sqrt{\log n}$  from (A3), then for any subset  $P \subseteq [p]$  and distribution  $\pi$  with support  $[0, 1]^p$  we have*

$$|c_{P,P_{\mathcal{X}}}(f) - c_{P,P_{\mathcal{X}}}(f_0)| \lesssim 4\sqrt{\log n} \|f - f_0\|_{2,P_{\mathcal{X}}}$$

where the empirical  $L_2$ -norm  $\|\cdot\|_{2,P_{\mathcal{X}}}$  is defined as  $\|f\|_{2,P_{\mathcal{X}}}^2 = n^{-1} \sum_{\mathbf{x} \in \mathcal{X}} |f(\mathbf{x})|^2$ .

**Corollary 3.5.** *Under the assumptions of Theorem 2 of [35] – Assumptions (A1), (A2), (A3), (A4), (A5), (A6), and (A7), and the prior assigned through (P1), (P2), and (P3) – and Theorem 3.4 above, there exist positive constants  $L_1$ ,  $L_2$ , and  $L_3$  such that*

$$\mathbb{E}_0 \Pi \left\{ (f, \sigma^2) : |V_{P,\pi}(f) - V_{P,\pi}(f_0)| + |\sigma^2 - \sigma_0^2| > L_1 \epsilon_n \sqrt{\log n} \mid Y_1, \dots, Y_n \right\} \rightarrow 0,$$

$$\mathbb{E}_0 \Pi \left\{ (f, \sigma^2) : |T_{j,\pi}(f) - T_{j,\pi}(f_0)| + |\sigma^2 - \sigma_0^2| > L_2 \epsilon_n \sqrt{\log n} \mid Y_1, \dots, Y_n \right\} \rightarrow 0,$$

$$\text{and } \mathbb{E}_0 \Pi \left\{ (f, \sigma^2) : |S_{j,\pi}(f) - S_{j,\pi}(f_0)| + |\sigma^2 - \sigma_0^2| > L_3 \epsilon_n \sqrt{\log n} \mid Y_1, \dots, Y_n \right\} \rightarrow 0$$

for  $\epsilon_n$  in (2.4).

The proofs of Theorem 3.4 and Corollary 3.5 can be obtained by replacing the random-design bound  $C_0^*$  with  $\sqrt{\log n}$  and the distribution  $\pi$  with the probability measure  $P_{\mathcal{X}}$ .

**4. Computation.** This section considers the computational tractability of estimating the Shapley values of the underlying regression function  $f_0$  for various fitted Bayesian surrogate models. Suppose each surrogate model is summarized by  $n_d$  post burn-in posterior draws. For each posterior draw  $i$ , denote the  $i$ th surrogate regression function as  $\hat{f}^{(i)}$ . For each input  $j \in [p]$ , we can estimate the  $j$ th Shapley effect  $S_{j,\pi}(f_0)$  of  $f_0$  by computing the  $n_d$  values of  $S_{j,\pi}(\hat{f}^{(i)})$ :

$$\begin{aligned} S_{j,\pi}(f_0) &\approx n_d^{-1} \sum_{i=1}^{n_d} S_{j,\pi}(\hat{f}^{(i)}) \\ &= n_d^{-1} \sum_{i=1}^{n_d} (p!)^{-1} \sum_{P \subseteq ([p] \setminus \{j\})} (p - |P| - 1)! |P|! [c_{P \cup \{j\},\pi}(\hat{f}^{(i)}) - c_{P,\pi}(\hat{f}^{(i)})]. \end{aligned}$$

But for each  $\hat{f}^{(i)}$ , computing the  $p$  Shapley effects would require computing the cost function (2.7) for  $2^p$  subsets of the set  $[p]$ . Using this approach for all inputs would thus require computing the cost function  $n_d \times 2^p$  times. The exponential increase in  $p$  is undesirable, but also the calculation of even a single cost function might be computationally intractable if  $p$  is large enough.

We first tackle the exponential increase in  $p$ . We can reduce the increase in  $p$  from exponential to linear by approximating the Shapley effect  $S_{j,\pi}(\hat{f}^{(i)})$  using the following permutation-based approach [2, 6]. For some chosen positive integer  $m$  and each posterior draw  $i$  and input  $j \in [p]$ , do the following  $m$  times: randomly draw a subset  $P \subseteq ([p] \setminus \{j\})$  by including each  $j' \in ([p] \setminus \{j\})$  in  $P$  with probability 0.5 (which gives each subset of  $([p] \setminus \{j\})$  equal probability  $2^{1-p}$  of being chosen) and then compute the difference  $c_{P \cup \{j\},\pi}(\hat{f}^{(i)}) - c_{P,\pi}(\hat{f}^{(i)})$  for the randomly drawn subset  $P$ . The mean over the  $m$  differences and  $n_d$  posterior draws is the desired estimate of the Shapley effect  $S_{j,\pi}(f_0)$ :

$$(4.1) \quad \hat{S}_{j,\pi,m} \left( \{\hat{f}^{(i)}\}_{i=1}^{n_d} \right) := n_d^{-1} \sum_{i=1}^{n_d} m^{-1} \sum_{l=1}^m \left[ c_{P_l^{(i)} \cup \{j\},\pi}(\hat{f}^{(i)}) - c_{P_l^{(i)},\pi}(\hat{f}^{(i)}) \right] \approx S_{j,\pi}(f_0),$$

where  $P_l^{(i)}$  is the  $l$ th of  $m$  randomly drawn subset of  $([p] \setminus \{j\})$  for the  $i$ th posterior draw. Hence this approach reduces the number of cost-function calculations from  $n_d \times 2^p$  to  $n_d \times p \times (2m)$ .

What value of  $m$  should be used? Both the computational cost and the accuracy of the surrogate-based Shapley-effect estimate increase with  $m \times n_d$ . Because any decent posterior summary of the surrogate model will require  $n_d$  to be at least somewhat large, we consider using a small value of  $m$  to keep the computational cost reasonable, but the random draws of subsets induce additional variability that will likely inflate the length of credible intervals (CIs) constructed for the Shapley-effect estimate. For the remainder of the article, we prioritize keeping computational cost low and hence use  $m = 1$ .

(As an aside, the relationship (2.9) implies for orthogonal designs that a CI for a Shapley effect should have length between the CI-length of the main-effects Sobol' index and the CI-length of the total-effects Sobol' index. Thus we can construct an approximate credible interval (CI) for the Shapley effect by giving it length equal to the average of the two Sobol' CI lengths and centering it at the Shapley-effect point estimate. Though we do not make use of it, this CI construction provides a rough sense of the posterior uncertainty of the Shapley-effect estimate without having to use  $m > 1$  if the inputs are orthogonal.)

We now consider how the each cost-function calculation is affected by which surrogate model is used. If the integrals in (2.7) have a closed-form expression, they can be computed exactly. For BART, a closed-form expression can be found using Theorem 1 of [34]. For Bayesian MARS, [21] provides a closed-form expression for estimating Sobol' indices and contains a numerical example with  $p = 200$ , but no posterior consistency results currently exist. For GP, a closed-form expression can be found for certain correlation functions, but these functions are typically restrictive i.e. assume stationarity and isotropy. If the cost function for  $\hat{f}^{(i)}$  is unavailable in closed form, the integrals can be approximated but the computation time will likely have to grow superlinearly in  $p$  to keep the resulting integral approximation error small. Because BART is the only surrogate model that is computationally tractable for moderate-to-large  $p$  and has theoretical guarantees of consistency for piecewise anisotropic

Var	Friedman			Morris			Bratley			g-function		
	23.8			5.25			0.057			3.076		
$j$	$V_j^*(f)$	$T_j^*(f)$	$S_j^*(f)$	$V_j^*(f)$	$T_j^*(f)$	$S_j^*(f)$	$V_j^*(f)$	$T_j^*(f)$	$S_j^*(f)$	$V_j^*(f)$	$T_j^*(f)$	$S_j^*(f)$
1	0.197	0.274	0.235	0.190	0.210	0.2	0.688	0.766	–	0.433	0.701	–
2	0.197	0.274	0.235	0.190	0.210	0.2	0.142	0.220	–	0.108	0.284	–
3	0.093	0.093	0.093	0.190	0.210	0.2	0.051	0.099	–	0.048	0.135	–
4	0.350	0.350	0.350	0.190	0.210	0.2	0.006	0.018	–	0.027	0.078	–
5	0.087	0.087	0.087	0.190	0.210	0.2	0.006	0.018	–	0.017	0.050	–

Table 1: Normalized main-effects  $V_j^*(f)$  and total-effects  $T_j^*(f)$  for various data-generating functions  $f$  and variable indices  $j \in [5]$  under orthogonal inputs. Normalized Shapley values  $S_j^*(f)$  for the Friedman and Morris functions can be found analytically and hence are provided. Shapley values for the Bratley and  $g$  functions are bounded between their respective main-effects and total-effects, per (2.9).

function spaces, the remainder of the article considers only BART as a surrogate model.

**5. Simulation study: orthogonal design.** This section explores the performance of BART-based Shapley values for moderate-to-large  $p$ , which is a regime where most other methods are computationally intractable. (The performance of BART-based Sobol’ indices is evaluated in detail in [34] and [39] and hence is not evaluated in this paper.) In particular, we illustrate how many posterior draws are needed for the BART-based Shapley effect estimates to converge to the underlying function’s Shapley effect. Datasets are generated using the following four test functions, which all depend on  $d = 5$  input variables:

1. The “Friedman” function [40] is defined as

$$f(\mathbf{x}) := 10 \sin(\pi x_1 x_2) + 20(x_3 - 0.5)^2 + 10x_4 + 5x_5.$$

2. The “Morris” function inspired by [41] is defined as

$$\begin{aligned} f(\mathbf{x}) &:= \alpha \sum_{i=1}^d x_i + \beta \sum_{i=1}^{d-1} x_i \sum_{j=i+1}^d x_j \\ &= \alpha(x_1 + x_2 + x_3 + x_4 + x_5) \\ &\quad + \beta(x_1 x_2 + x_1 x_3 + x_1 x_4 + x_1 x_5 + x_2 x_3 + x_2 x_4 + x_2 x_5 + x_3 x_4 + x_3 x_5 + x_4 x_5) \end{aligned}$$

where  $\alpha = \sqrt{12} - 6\sqrt{0.1(d-1)} \approx -0.331$  and  $\beta = \frac{12}{\sqrt{10(d-1)}} \approx 1.897$  are chosen.

3. The “Bratley” function [42, 43] is defined as

$$f(\mathbf{x}) := \sum_{i=1}^d (-1)^i \prod_{j=1}^i x_j = -x_1 + x_1 x_2 - x_1 x_2 x_3 + x_1 x_2 x_3 x_4 - x_1 x_2 x_3 x_4 x_5.$$

4. The “ $g$ -function” from [44] is defined as

$$f(\mathbf{x}) := \prod_{k=1}^d \frac{|4x_k - 2| + c_k}{1 + c_k},$$

where we use the coefficient values  $c_k = (k-1)/2$  for  $k = 1, \dots, d$  suggested by [45].

Table 1 contains the variances, Sobol' indices, and Shapley values for each test function.

For our first set of explorations, we create a dataset with  $n = 50p$  observations and noise variance  $\sigma_0^2 = 1$  from (2.1) for each test function and each  $p \in \{5, 50, 200\}$ . To each of the twelve datasets, we fit a BART model with  $n_d = 1000$  posterior draws and 200 trees with code from [46]. For each fitted BART model, we compute Shapley-effect running means  $\hat{S}_{j,\pi,1}(\{\hat{f}^{(i)}\}_{i=1}^k)$  for each  $k \in [n_d]$  and each  $j \in [d]$ , where  $\hat{S}_{j,\pi,1}(\{\hat{f}^{(i)}\}_{i=1}^k)$  is defined in (4.1). The running means, displayed in Figure 2, are shown to stabilize before  $k = 150$  for all tested functions and values of  $p$ , which implies a much smaller value of  $n_d$  could have been used to obtain a practically identical Shapley-effect estimate. The running means also stabilize close to the true Shapley effects for the Friedman and Morris functions with either  $(p, n) = (50, 2500)$  or  $(p, n) = (200, 10000)$ . This  $p = 200$  result becomes even more notable if we consider the fitted BART models do not use (P1)'s tree prior with Dirichlet sparsity from [30]. But for the Bratley and  $g$  functions, the running means stabilize often far from the true Shapley effects. In particular, the largest Shapley effect for each of these two functions is consistently and largely underestimated. The Friedman and Morris functions differ from the Bratley and  $g$  functions in that the former two functions have at most a two-way interaction, whereas the latter two functions each contain a multiplicative product of (univariate functions of) all  $d = 5$  active inputs.

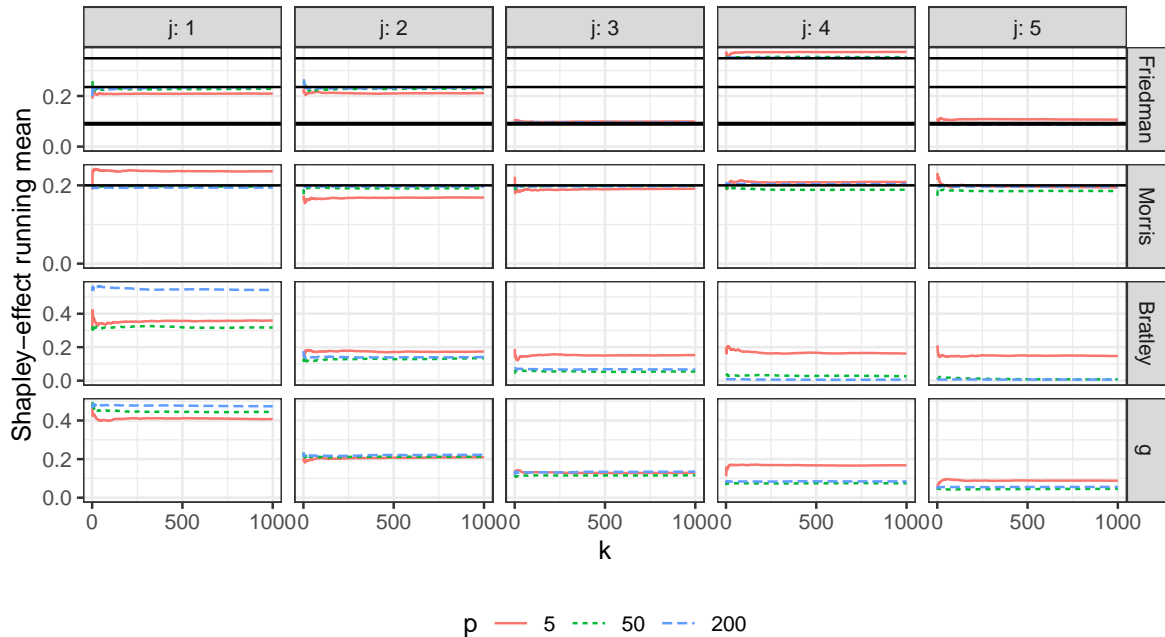


Figure 2: BART-based Shapley-effect running means  $\hat{S}_{j,\pi,1}(\{\hat{f}^{(i)}\}_{i=1}^k)$ , defined in (4.1), for each  $k \in [1000]$  and four test functions. For the Friedman and Morris functions, the dark horizontal lines indicate the true Shapley effects.

For the more challenging Bratley and  $g$  functions, we next explore what parameters or

priors should be changed for the running means to stabilize closer to the true Shapley effects. Of the three directions we explored – increasing the number of trees to 300, weakening the tree-depth prior to encourage higher order interactions, and increasing  $n$  – only the third (with 200 trees, the same tree-depth prior as in the first set of explorations, and  $p = 5$ ) yielded running means that stabilized closer to the true Shapley effects (see Figure 3). This provides assurance that for these more challenging functions, the running means can stabilize close to the true Shapley effects if  $n$  is large enough without having to change any other parameters or priors.

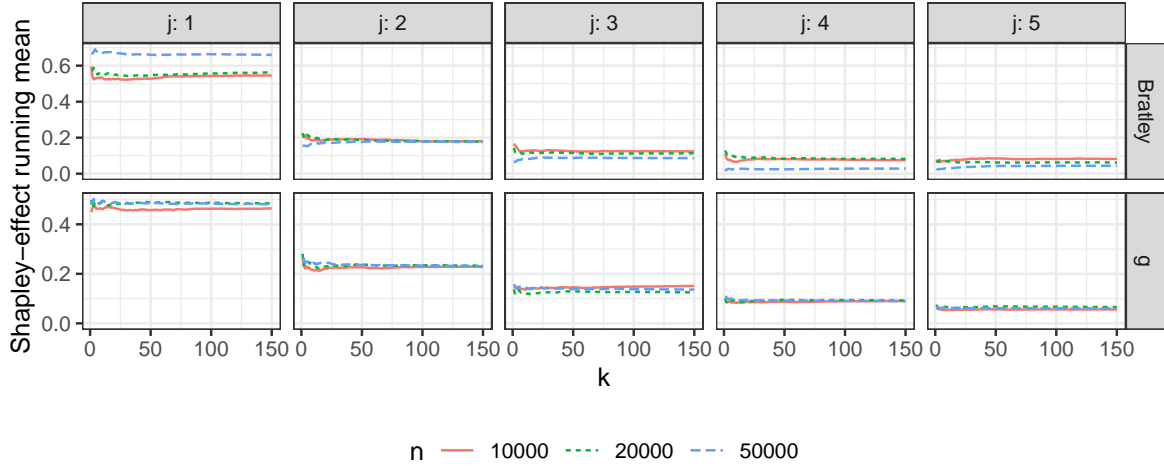


Figure 3: BART-based Shapley-effect running means  $\hat{S}_{j,\pi,1}(\{\hat{f}^{(i)}\}_{i=1}^k)$ , defined in (4.1), for each  $k \in [150]$  and two test functions.

**6. Discussion.** This article establishes posterior contraction rates for Sobol’ index and Shapley effect estimators computed using BART. The proofs of our contraction rates required proving a property similar to Lipschitz continuity for Sobol’ indices and Shapley effects before using recent contraction-rate results that applies to function spaces with heterogeneous smoothness and sparsity in high dimensions and to fixed and random designs. This article also illustrates the computational tractability and performance of BART-based Shapley effects on four different test functions under orthogonal inputs and moderate-to-large  $p$ . Code to fit BART models and compute Sobol’ index and Shapley effect estimates is found in [46].

Regarding computation, it is challenging to encode an arbitrary (e.g. nonorthogonal) input design with full support into a BART model. This can be possibly achieved by replacing the volume of each hyperrectangle used to compute BART-based Sobol’ indices and Shapley effects with the proportion of observations that fall in each hyperrectangle. A direction for future work is to implement the calculation of BART-based Shapley effects under an arbitrary (e.g. nonorthogonal) input design and evaluate its performance.

Another direction of future work is to establish posterior contraction rates for estimators computed from a GP metamodel. Chapter 11 of [37] contains contraction rates for GP random

functions under various correlation functions. Given that closed-form expressions for GP-based Sobol' indices are established for certain correlation functions, it is possible that a strategy similar to the one used in this article can be used to establish contraction rates for GP-based Sobol' indices and Shapley effects.

Finally, one could also try to establish posterior consistency and contraction rates for estimators of other sensitivity indices computed using BART. An example is the Cramér-von-Mises index [47], which is based on the whole distribution of the random variable rather than on only the second moment. Another option is a sensitivity index geared toward causal inference, per the field's growing use of BART [48].

**Acknowledgments.** AH would like to acknowledge Miheer Dewaskar for fruitful discussions. The work of MTP was supported in part by the National Science Foundation under Agreements DMS-1916231, OAC-2004601, and in part by the King Abdullah University of Science and Technology (KAUST) Office of Sponsored Research (OSR) under Award No. OSR-2018-CRG7-3800.3.

### References.

- [1] Il'ya Meerovich Sobol'. On sensitivity estimation for nonlinear mathematical models. *Matematicheskoe modelirovanie*, 2(1):112–118, 1990.
- [2] Eunhye Song, Barry L Nelson, and Jeremy Staum. Shapley effects for global sensitivity analysis: Theory and computation. *SIAM/ASA Journal on Uncertainty Quantification*, 4(1):1060–1083, 2016.
- [3] Lloyd S. Shapley. A value for n-person games. Technical report, The RAND Corporation, 1952.
- [4] Art B Owen. Sobol' indices and shapley value. *SIAM/ASA Journal on Uncertainty Quantification*, 2(1):245–251, 2014.
- [5] Nazih Benoumechiara and Kevin Elie-Dit-Cosaque. Shapley effects for sensitivity analysis with dependent inputs: bootstrap and kriging-based algorithms. *ESAIM: Proceedings and Surveys*, 65:266–293, 2019.
- [6] Baptiste Broto, François Bachoc, and Marine Depecker. Variance reduction for estimation of shapley effects and adaptation to unknown input distribution. *SIAM/ASA Journal on Uncertainty Quantification*, 8(2):693–716, 2020.
- [7] Elmar Plischke, Giovanni Rabitti, and Emanuele Borgonovo. Computing shapley effects for sensitivity analysis. *SIAM/ASA Journal on Uncertainty Quantification*, 9(4):1411–1437, 2021.
- [8] Thomas J Santner, Brian J Williams, and William I Notz. *The Design and Analysis of Computer Experiments, Second Edition*. Springer-Verlag, 2018.
- [9] Jeremy E Oakley and Anthony O'Hagan. Probabilistic sensitivity analysis of complex models: a Bayesian approach. *Journal of the Royal Statistical Society: Series B (Statistical Methodology)*, 66(3):751–769, 2004.
- [10] Wei Chen, Ruichen Jin, and Agus Sudjianto. Analytical variance-based global sensitivity analysis in simulation-based design under uncertainty. *Journal of mechanical design*, 127(5):875–886, 2005.
- [11] Wei Chen, Ruichen Jin, and Agus Sudjianto. Analytical global sensitivity analysis and



- uncertainty propagation for robust design. *Journal of quality technology*, 38(4):333–348, 2006.
- [12] Amandine Marrel, Bertrand Iooss, Beatrice Laurent, and Olivier Roustant. Calculations of Sobol’ indices for the Gaussian process metamodel. *Reliability Engineering & System Safety*, 94(3):742–751, 2009.
- [13] Hyejung Moon. *Design and analysis of computer experiments for screening input variables*. PhD thesis, The Ohio State University, 2010.
- [14] Joshua Svenson, Thomas Santner, Angela Dean, and Hyejung Moon. Estimating sensitivity indices based on gaussian process metamodels with compactly supported correlation functions. *Journal of Statistical Planning and Inference*, 144:160–172, 2014.
- [15] Bertrand Iooss and Clémentine Prieur. Shapley effects for sensitivity analysis with correlated inputs: comparisons with sobol’ indices, numerical estimation and applications. *International Journal for Uncertainty Quantification*, 9(5), 2019.
- [16] Bruno Sudret. Global sensitivity analysis using polynomial chaos expansions. *Reliability engineering & system safety*, 93(7):964–979, 2008.
- [17] Robert B. Gramacy and Matthew Taddy. Categorical inputs, sensitivity analysis, optimization and importance tempering with tgp version 2, an R package for treed Gaussian process models. *Journal of Statistical Software*, 33(6):1–48, 2010.
- [18] Robert B Gramacy, Matt Taddy, Stefan M Wild, et al. Variable selection and sensitivity analysis using dynamic trees, with an application to computer code performance tuning. *The Annals of Applied Statistics*, 7(1):51–80, 2013.
- [19] Zeping Wu, Donghui Wang, Patrick Okolo, Fan Hu, and Weihua Zhang. Global sensitivity analysis using a gaussian radial basis function metamodel. *Reliability Engineering & System Safety*, 154:171–179, 2016.
- [20] Shuang Li, Bin Yang, and Fei Qi. Accelerate global sensitivity analysis using artificial neural network algorithm: Case studies for combustion kinetic model. *Combustion and Flame*, 168:53–64, 2016.
- [21] Devin Francom, Bruno Sansó, Ana Kupresanin, and Gardar Johannesson. Sensitivity analysis and emulation for functional data using bayesian adaptive splines. *Statistica Sinica*, pages 791–816, 2018.
- [22] Majdi I Radaideh and Tomasz Kozłowski. Surrogate modeling of advanced computer simulations using deep gaussian processes. *Reliability Engineering & System Safety*, 195:106731, 2020.
- [23] Sébastien Da Veiga and Fabrice Gamboa. Efficient estimation of sensitivity indices. *Journal of Nonparametric Statistics*, 25(3):573–595, 2013.
- [24] Alexandre Janon, Thierry Klein, Agnes Lagnoux, Maëlle Nodet, and Clémentine Prieur. Asymptotic normality and efficiency of two sobol index estimators. *ESAIM: Probability and Statistics*, 18:342–364, 2014.
- [25] Fabrice Gamboa, Pierre Gremaud, Thierry Klein, and Agnès Lagnoux. Global sensitivity analysis: A novel generation of mighty estimators based on rank statistics. *Bernoulli*, 28(4):2345–2374, 2022.
- [26] Hugh A Chipman, Edward I George, and Robert E McCulloch. Bart: Bayesian additive regression trees. *The Annals of Applied Statistics*, 4(1):266–298, 2010.
- [27] Hugh Chipman, Pritam Ranjan, and Weiwei Wang. Sequential design for computer

- experiments with a flexible Bayesian additive model. *Canadian Journal of Statistics*, 40(4):663–678, 2012.
- [28] Robert B Gramacy and Benjamin Haaland. Speeding up neighborhood search in local Gaussian process prediction. *Technometrics*, 58(3):294–303, 2016.
- [29] Akira Horiguchi, Thomas J Santner, Ying Sun, and Matthew T Pratola. Using bart to perform pareto optimization and quantify its uncertainties. *Technometrics*, pages 1–11, 2022.
- [30] Antonio R. Linero. Bayesian regression trees for high-dimensional prediction and variable selection. *Journal of the American Statistical Association*, 113(522):626–636, 2018.
- [31] Stéphanie van der Pas and Veronika Ročková. Bayesian dyadic trees and histograms for regression. In I. Guyon, U. V. Luxburg, S. Bengio, H. Wallach, R. Fergus, S. Vishwanathan, and R. Garnett, editors, *Advances in Neural Information Processing Systems 30*, pages 2089–2099. Curran Associates, Inc., 2017.
- [32] Yi Liu, Veronika Ročková, and Yuexi Wang. Abc variable selection with Bayesian forests. *arXiv preprint arXiv:1806.02304*, 2021.
- [33] Saman Razavi, Anthony Jakeman, Andrea Saltelli, Clémentine Prieur, Bertrand Iooss, Emanuele Borgonovo, Elmar Plischke, Samuele Lo Piano, Takuya Iwanaga, William Becker, et al. The future of sensitivity analysis: an essential discipline for systems modeling and policy support. *Environmental Modelling & Software*, 137:104954, 2021.
- [34] Akira Horiguchi, Matthew T Pratola, and Thomas J Santner. Assessing variable activity for bayesian regression trees. *Reliability Engineering & System Safety*, 207:107391, 2021.
- [35] Seonghyun Jeong and Veronika Ročková. The art of bart: On flexibility of bayesian forests. *arXiv preprint arXiv:2008.06620*, 2022.
- [36] Hugh A. Chipman, Edward I. George, and Robert E. McCulloch. BART: Bayesian additive regression trees. *The Annals of Applied Statistics*, 4:266–298, 2010.
- [37] Subhashis Ghosal and Aad Van der Vaart. *Fundamentals of nonparametric Bayesian inference*, volume 44. Cambridge University Press, 2017.
- [38] Il’ya Meerovich Sobol’. Sensitivity estimates for nonlinear mathematical models. *MMCE*, 1(4):407–414, 1993.
- [39] Akira Horiguchi. *Bayesian Additive Regression Trees: Sensitivity Analysis and Multiobjective Optimization*. PhD thesis, The Ohio State University, 2020.
- [40] Jerome H Friedman. Multivariate adaptive regression splines. *The annals of statistics*, 19(1):1–67, 1991.
- [41] Max D Morris, Leslie M Moore, and Michael D McKay. Sampling plans based on balanced incomplete block designs for evaluating the importance of computer model inputs. *Journal of Statistical Planning and Inference*, 136(9):3203–3220, 2006.
- [42] Paul Bratley, Bennett L Fox, and Harald Niederreiter. Implementation and tests of low-discrepancy sequences. *ACM Transactions on Modeling and Computer Simulation (TOMACS)*, 2(3):195–213, 1992.
- [43] Sergei Kucherenko, Balazs Feil, Nilay Shah, and Wolfgang Mauntz. The identification of model effective dimensions using global sensitivity analysis. *Reliability Engineering & System Safety*, 96(4):440–449, 2011.
- [44] Andrea Saltelli and Ilya M Sobol’. About the use of rank transformation in sensitivity analysis of model output. *Reliability Engineering & System Safety*, 50(3):225 – 239, 1995.

- 
- [45] Thierry Crestaux, Olivier Le Maître, and Jean-Marc Martinez. Polynomial chaos expansion for sensitivity analysis. *Reliability Engineering & System Safety*, 94(7):1161 – 1172, 2009. Special Issue on Sensitivity Analysis.
- [46] Matthew T. Pratola. Open Bayesian trees, 2023. <https://bitbucket.org/mpratola/openbt/src/master/>. Accessed: 2023-04-03.
- [47] Fabrice Gamboa, Thierry Klein, and Agnès Lagnoux. Sensitivity analysis based on cramér–von mises distance. *SIAM/ASA Journal on Uncertainty Quantification*, 6(2):522–548, 2018.
- [48] P Richard Hahn, Jared S Murray, and Carlos M Carvalho. Bayesian regression tree models for causal inference: Regularization, confounding, and heterogeneous effects (with discussion). *Bayesian Analysis*, 15(3):965–1056, 2020.